Challenges and Limits of Extended Kalman Filter based Sensorless Control of Permanent Magnet Synchronous Machine Drives

Zdeněk Peroutka[1], Václav Šmídl[2] and David Vošmik[1]

[1]UNIVERSITY OF WEST BOHEMIA IN PILSEN
Univerzitní 8, 306 14
Plzeň, Czech Republic
Tel.: +420 / 37763-4443 (-4446).
Fax: +420 / 37763 4402.
E-Mail: peroutka@ieee.org, vosmik1@kev.zcu.cz
URL: http://www.fel.zcu.cz

[2]INSTITUTE OF INFORMATION THEORY AND AUTOMATION
ACADEMY OF SCIENCE OF THE CZECH REPUBLIC
Pod vodárenskou věží 4, 182 08
Prague, Czech Republic
Tel.: +420 / 266 052 420.
Fax: +420 / 266 052 068.
E-Mail: smidl@utia.cas.cz
URL: http://www.utia.cz

Acknowledgements

Keywords

Control of Drive, Estimation technique, Intelligent drive, Permanent magnet motor, Sensorless control.

Abstract

A sophisticated simulator of permanent magnet synchronous machine (PMSM) drive was developed and is used for research into model-based sensorless control strategies. In this paper, we focus on estimators based on the extended Kalman Filter (EKF). The limits and possible improvements of the EKF are investigated using the developed simulator and real data recorded on designed laboratory prototypes of PMSM drives. From the viewpoint of possible improvement of the estimator, the main attention has been paid to the following phenomena: (i) uncertainty of a stator voltage vector (effects of dead-times, non-linear voltage drops on power devices, etc.), (ii) impact of imperfect model discretization, and (iii) impact of unknown load torque. These phenomena are analyzed and the results are used to tune covariance matrices of the EKF via a semi-analytical approach. Theoretical results are verified by experiments made on two developed prototypes of PMSM drive of rated power of 10.7kW and 310W. Finally, this paper summarizes the major limits of EKF and proposes prospective ways for further research leading to reduction of these limits.

Introduction

This research was motivated by demand of our industrial partners for proposal of a prospective sensorless control strategy for permanent magnet synchronous machine (PMSM) drives operated in modern transport systems. The sensorless control of PMSM drives is well established and discussed in the literature. Several interesting papers and books covering this issue were published, e.g. [1]. However, this problem is still open for further research. Specifically, sensorless operation of the drive in standstill and in low speeds is not satisfactorily resolved. We have focused in the first part of our research on model-based sensorless techniques. One of our important tasks was to design a model of

the drive that would allow for better control performance in very low speeds. The resulting model is then estimated using the extended Kalman Filter (EKF). This filter is well known in the area, its design considerations and implementation in sensorless control of PMSM drives were discussed e.g. in [1], [2] – [5]. The EKF is often considered to be an excessively complex algorithm, which is difficult to implement (especially in the case of fixed-point application) and requires huge computational performance. However, this disadvantage can be avoided using either manually optimized EKF equations (such as in our case) or various kinds of square-root algorithms (e.g. [6]). Another well-known disadvantage is the need for tuning of covariance matrices of the EKF, as discussed e.g. in [5]. This paper complements empirical findings and recommendations of [5] by a theoretical study of the problem using the developed sophisticated simulator.

The EKF is an approximate technique for Bayesian filtering of non-linear models with Gaussian noises. It is known to work well when the nonlinearities are not severe and the distribution of the disturbances is mutually independent zero-mean Gaussian with known variance. When these conditions are not met, the filter is known to fail [7]. However, experimental evidence suggests that EKF is an adequate choice for sensorless control of PMSM when properly tuned – e.g. [2], [3]. Nevertheless, the limits of EKF in these applications are not exactly known. Therefore, the aim of this paper is to analyze optimal conditions and settings for the EKF. The challenge is to design a valid stochastic model of the PMSM drive that meets the requirements of the EKF. The most challenging is modeling of the disturbances; we intend to assure that the disturbances have: (i) zero mean, (ii) temporal independence, and (iii) known fixed variance. Standard model of the PMSM drive is studied in the light of these requirements. Specifically, the following phenomena are addressed: (I) uncertainty of reconstructed stator voltage vector (effects of dead-times, non-linear voltage drops on power electronics devices, etc.), (II) impact of imperfect model discretization, and (III) impact of unknown load torque. The findings are used for tuning of covariance matrices of the EKF.

This paper is organized as follows. First, the developed sophisticated simulator of a PMSM drive is presented. Second, a stochastic model of a PMSM drive is analyzed and its possible improvements are discussed. Third, the theoretical results provided in this paper are verified by experiments made on two developed PMSM drives of rated power of 10.7kW and 310W. Finally, major constrains and limits of the EKF are summarized and prospective ways for further research leading to reduction of the EKF limits are discussed.

Identification and Control Simulator based on BDM Environment

In order to understand cooperation of the EKF and the PMSM drive, we have built a sophisticated simulator which allows us to model internal state of the drive in detail. This knowledge serves for improvements of stochastic state-space model of the drive. Valid stochastic model can be used for tuning of covariance matrices in the EKF which is our current goal. Since EKF can be interpreted as a special case of Bayesian filtering [8], we have designed our simulator in the Bayesian Decision Making (BDM) development environment. Furthermore, the verified stochastic drive model can be used for application of more advanced Bayesian filtering techniques which are already implemented in BDM (such as particle or unscented filter) – this is our research direction.

Developed Bayesian Decision Making (BDM) Environment

BDM has been developed as a unified framework for development of identification and control techniques based on stochastic models. Following the Bayesian approach, all uncertainty within the model is modeled by probability density functions. The basic building blocks of the framework are thus probability density functions, Bayesian estimators and stochastic controllers which operate on data provided by data-sources. These blocks are implemented as classes in object-oriented design. Hence, the existing filters and data sources can be easily extended for new models, simulators or real-time physical processes. The framework allows easy combination of various estimation methods and offers tools for their mutual comparison. It is being developed as an open-source product available from our web site http://mys.utia.cas.cz:1800/trac/bdm under the GPL license.

Block configuration of the developed simulator is shown in Fig. 1. Here, the data source for the EKF estimator is represented by "physical" model of PMSM drive. For experiments with real measurements, data recorded on PMSM drive prototypes are used as a data source.
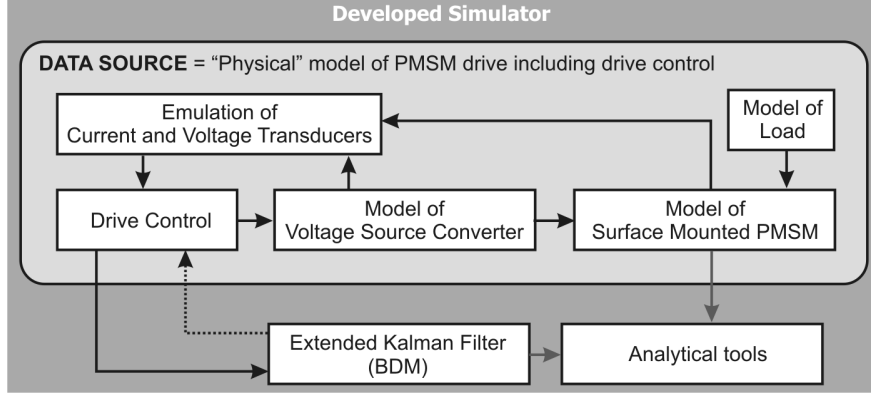
Fig. 1: Block scheme of developed simulator within BDM framework

"Physical" model of permanent magnet synchronous motor drive: BDM data source

This model of surface mounted PMSM drive uses conventional rotor flux oriented vector control in Cartesian coordinates for control of the investigated drive (see Fig. 2). Simulator uses carrier-based PWM and voltage source inverter model which respects as close as possible dead-time effects and non-linear voltage drops on power electronics devices (the power devices are modeled using approximations of their V-A characteristics). Control strategy respects behavior of a real microcontroller based control system including realistic sampling, known transport delays and finite calculation times.

Surface mounted PMSM is modeled using the conventional continues-time model in the stationary reference frame:

$$
\begin{aligned}
\frac{di_{s\alpha}}{dt} &= -\frac{R_s}{L_s}i_{s\alpha} + \frac{\Psi_{PM}}{L_s}\omega_{me}\sin\vartheta_e + \frac{u_{s\alpha}}{L_s}, \\
\frac{di_{s\beta}}{dt} &= -\frac{R_s}{L_s}i_{s\beta} - \frac{\Psi_{PM}}{L_s}\omega_{me}\cos\vartheta_e + \frac{u_{s\beta}}{L_s}, \\
\frac{d\omega_{me}}{dt} &= \frac{k_p p_p^2 \Psi_{PM}}{J}\left(i_{s\beta}\cos\vartheta_e - i_{s\alpha}\sin\vartheta_e\right) - \frac{B}{J}\omega_{me} - \frac{p_p}{J}T_L, \\
\frac{d\vartheta_e}{dt} &= \omega_{me}.
\end{aligned}
\tag{1}
$$

Here $i_{s\alpha}$, $i_{s\beta}$, $u_{s\alpha}$ and $u_{s\beta}$ represent components of stator current and voltage vectors in the stationary reference frame, respectively; ω_{me} is electrical rotor speed and ϑ_e is position of rotor flux vector in the stationary reference frame (the rotor flux vector position in stationary frame is in case of PMSM equal to electrical rotor position). R_s and L_s is stator resistance and inductance respectively, Ψ_{PM} is the flux linkage excited by permanent magnets on the rotor, B is friction, T_L is load torque, J is moment of inertia, p_p is number of pole pairs and k_p is the Park constant. For further research we have also prepared model of permanent magnet motor in revolving reference frame linked to the rotor flux vector which is eligible particularly for research into interior permanent magnet motor types. Both PMSM models are calculated in discrete form using Adams-Bashforth difference formula of 4th order with sampling period of 1μs.

Stochastic Model of PMSM Drive

The EKF is an approximate solution of Bayesian filtering for a non-linear state-space model with Gaussian disturbances

$$
\begin{aligned}
x_t &= g(x_{t-1}, u_t) + e_t, \quad p(e_t) = N(0, Q), \\
y_t &= h(x_t, u_t) + \varepsilon_t, \quad p(\varepsilon_t) = N(0, R),
\end{aligned}
\tag{2}
$$

where $g()$ and $h()$ are non-linear functions, $p(e_t)$ denotes probability density function of disturbance e_t, $N(0,Q)$ denotes Gaussian distribution with zero mean value and covariance matrix Q.
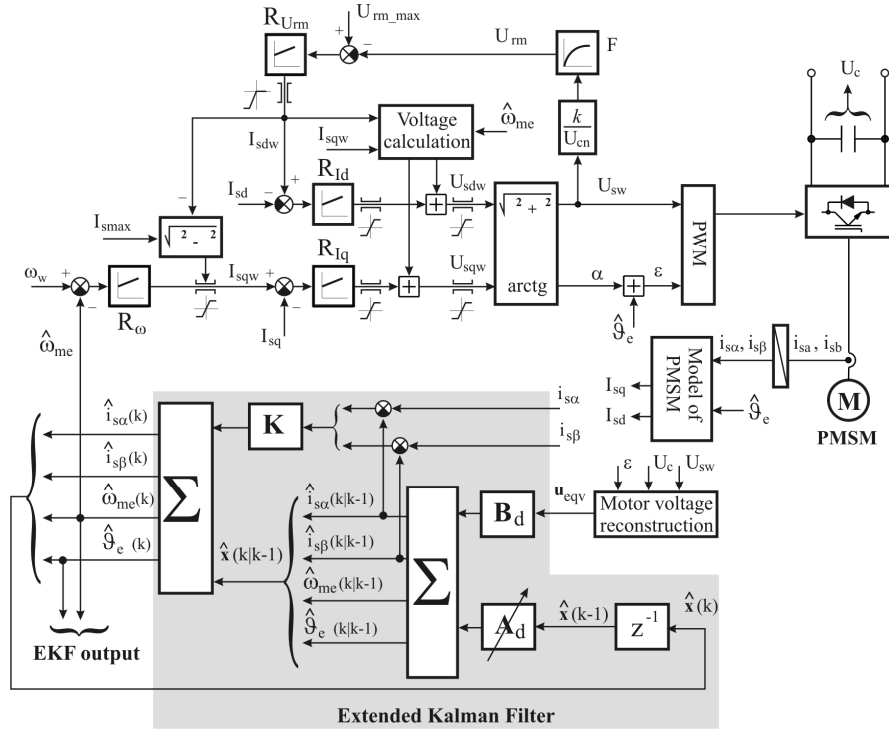
Fig. 2: Configuration of investigated sensorless control of PMSM drive

EKF is an approximation of the exact Bayesian filtering for the above model projecting the posterior density of x_t into a Gaussian, $p(x_t \mid y_1...y_t) = N(\hat{x}_t, P_t)$, this approximation is using linearization of the non-linear function $g()$ at working point $\hat{x}_t$. EKF performs well when: (i) the Gaussian assumption is met, and (ii) working point $\hat{x}_t$ is close to the true state x_t.

Discrete-time state-space model of the PMSM drive can be obtained from (1) using Euler approximation of the first order. Under assumption that the rotor speed change is negligible within the sampling period, the discrete-time state-space model is given by:

$$i_{s\alpha}(t+1) = \left(1 - \frac{R_s}{L_s}\Delta t\right)i_{s\alpha}(t) + \frac{\Psi_{PM}}{L_s}\Delta t\omega_{me}(t)\sin\vartheta_e(t) + \frac{\Delta t}{L_s}u_{s\alpha}(t),$$

$$i_{s\beta}(t+1) = \left(1 - \frac{R_s}{L_s}\Delta t\right)i_{s\beta}(t) - \frac{\Psi_{PM}}{L_s}\Delta t\omega_{me}(t)\cos\vartheta_e(t) + \frac{\Delta t}{L_s}u_{s\beta}(t),$$

$$\omega_{me}(t+1) = \omega_{me}(t),$$

$$\vartheta_e(t+1) = \vartheta_e(t) + \Delta t\omega_{me}(t).$$

(3)

Here, Δt is the chosen sampling period. Equation (3) defines function $g()$ under assignments: $x_t = [i_{s\alpha};$ $i_{s\beta}; \omega_{me}; \vartheta_e]$, $u_t = [u_{s\alpha}; u_{s\beta}]$, where $u_{s\alpha}$ and $u_{s\beta}$ are components of the stator voltage vector. Function $h()$ for this model is trivial, since measurements of state variables $i_{s\alpha}$ and $i_{s\beta}$ are unbiased. Hence,

$$h(x_t, u_t) = \begin{bmatrix} 1 & 0 & 0 & 0 \\ 0 & 1 & 0 & 0 \end{bmatrix} x_t + \varepsilon_t.$$

(4)

It remains to specify covariance matrices Q and R. These matrices represent statistical properties of disturbances e_t and ε_t, which accumulate all uncertainty in the model. We consider the following sources of uncertainty in the model:

1. Measurement error.
2. Uncertainty of reconstructed stator voltage vector (effects of dead-times, non-linear voltage drops on power devices, etc.).
3. Impact of imperfect model discretization – error in discretization of the model (1) due to the used first-order Euler method.

4. Impact of unknown load torque and generally mechanical equation in EKF model.
5. Unknown parameters of motor equivalent circuit and variation of these parameters.

Remark 1: The EKF requires all disturbances to be modeled as Gaussian. Thus, other probability densities must be approximated by a Gaussian. We will use minimization of Kullback-Leibler divergence from the approximated density to the Gaussian density for this task. The resulting Gaussian has the first two moments equal to those of the approximated density. For example, a uniform probability density on interval [a,b] will be approximated by a Gaussian with mean value (a+b)/2 and variance $(b-a)^2/12$, i.e. $N((a+b)/2, (b-a)^2/12)$.

Measurement error

The components of stator current vector $i_{s\alpha}$, $i_{s\beta}$ are observed via A/D converter with discretization step Δi (we of course measure the phase currents i_{sa}, i_{sb} which are then transformed to the space vector in stationary reference frame). Since this error is the only source of disturbance for the observation equation, we can consider ε_t to be uniformly distributed on interval $[-\Delta i/2, \Delta i/2]$. Hence, the optimal Gaussian density (Remark 1) has zero mean and variance $\Delta i^2/12$. In our particular case, the discretization step is $\Delta i = 0.085$A. The optimal matrix R for this A/D converters is then $R = \mathrm{diag}(0.0006, 0.0006)$.

An input to the stochastic model of PMSM (3) is the stator voltage vector in stationary reference frame. Direct measurement of the motor voltage by voltage transducers is problematic, because the motor voltage generated by voltage source converter consists of voltage pulses. Therefore, the components of the motor voltage vector are estimated indirectly based on the demanded voltage magnitude, demanded position of motor voltage vector in stationary reference frame and measured converter dc-link voltage. The measurement of dc-link voltage is influenced by discretization error Δu. The Gaussian probability density of this error can be derived using the same approach as for current measurement error Δi. Furthermore, the conventional reconstruction of motor voltage vector does not respect the impact of dead-times and non-linear voltage drops on power electronics devices. The impact of the motor voltage estimation error on the EKF estimator performance is going to be explored in the following section.

Uncertainty of reconstructed stator voltage vector: effects of dead-times and non-linear voltage drops on power electronics devices

The reconstructed motor voltage vector (u_{eqv}), which is the input to the stochastic model (3), is influenced by the following disturbances: (i) error of converter dc-link voltage measurement, (ii) dead-times and (iii) non-linear voltage drops on power electronics devices. These phenomena contribute to the voltage error Δu_{eqv} having impact on the first two equations of (3). The error Δu_{eqv} influences disturbance e_t and its covariance matrix Q. Dead-times and voltage drops, which are the major problem, take effect on a very short time scale compared to the sampling period of both the controller and the EKF estimator. Their effect on the time scale of the sampling period can be studied only via statistical properties. While mean value of the error can be predicted, its variance must be studied in simulation. The relation between the "real" voltage vector on the motor terminals ($u_s = [u_{s\alpha}; u_{s\beta}]$) and the conventionally reconstructed motor voltage vector ($u_{eqv} = [u_{s\alpha\_eqv}; u_{s\beta\_eqv}]$) is given by:

$$u_{s\alpha} = u_{s\alpha\_eqv} - \Delta u_{s\alpha,VA} - \Delta u_{s\alpha,DT} - \Delta u_{s\alpha,ADC}$$
$$u_{s\beta} = u_{s\beta\_eqv} - \Delta u_{s\beta,VA} - \Delta u_{s\beta,DT} - \Delta u_{s\beta,ADC} \quad . \tag{5}$$

Here, $\Delta u_{s,VA}$ is the voltage drop on power devices, $\Delta u_{s,DT}$ is the difference caused by dead-time and $\Delta u_{s,ADC}$ is the difference caused by error of dc-link voltage measurement.

The error $\Delta u_{s,VA}$ is given by the VA characteristics of power electronics devices employed in the voltage source converter. The voltage drops depend on several factors – these are particularly the motor phase currents and power devices chip temperatures. Since measurements of motor phase currents are available and the converter switching diagram is known, we derived a simplified formula for estimation of voltage drops $\Delta u_{s,VA}$ (the similar approach is used e.g. in [9]). The approximate voltage drop in each converter phase in the given sampling instant is:

$$\Delta u_{x,VA} = \left(\left|i_{x,t}\right| > i_{trh}\right)u_{trh}\,sign\!\left(i_{x,t}\right) + R_d i_{x,t}, \tag{6}$$

where $x = (a,b,c)$ denotes motor phase, $i_{x,t}$ is the current in phase x, i_{trh} is a threshold current (it represents non-sensitivity band around zero current), R_d is the equivalent resistance of the power device and u_{trh} is a threshold voltage of the given power device. The voltage drops in phase coordinates are transformed to the stationary Cartesian coordinates and in this way, the corrected components of stator voltage vector ($u_{s\alpha\_eqv\_comp}$, $u_{s\beta\_eqv\_comp}$) are calculated.

Variance of this error was studied in simulation for the 10.7kW drive with parameters of the compensation ($i_{trh} = 0.3$A, $u_{trh} = 1.4$V). The simulation results are displayed in Fig. 3.
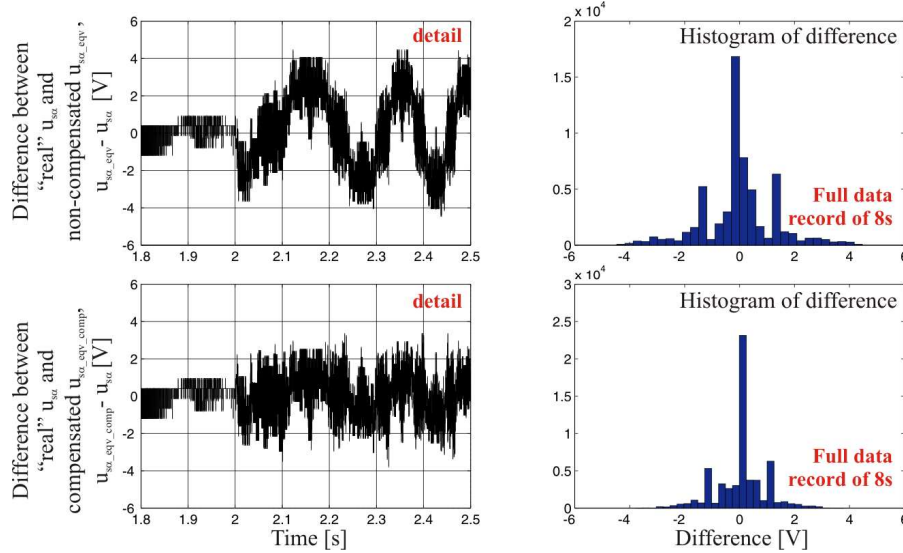

Fig 3. Motor voltage vector reconstruction error. **Left**: differences between "real" and reconstructed motor voltage. **Right**: Histograms of the error for all simulation of lengths 8s.
Top: conventional voltage vector reconstruction. **Bottom**: voltage vector reconstruction with proposed compensation. Data source: simulator; speed profile + load torque profile.

After compensation, the histogram of errors in Fig. 3 (bottom right) corresponds well to a Gaussian density, with the exception of sharp peaks around zero and ±1.2V. The former peak is a result of a standstill period in the simulation; the latter corresponds to the discretization error mentioned above. Without these peaks, the histogram can be considered to represent realizations of Gaussian density $N(0,1)$. This disturbance contributes to e_t by term $\Delta u_{eqv}\Delta t/L_s$, the variance of this contribution being $(\Delta t/L_s)^2$. This term will be denoted q_{pwm}.

Impact of imperfect model discretization

The error of model discretization was studied by comparison of the continuous-time model integrated on fine time-scale of 1μs with the discrete model with sampling period of 125 μs. Differences between these two models for the 10.7kW drive are displayed in Fig. 4, in tandem with their histograms. Note that the error of integration is systematic (temporally correlated). Hence, it could be compensated, e.g. by means of higher-order discretization. Most significant systematic deviation is in ϑ_e which could be easily compensated using derivative of ω_{me}. However, the contribution of this type of error to the total disturbance is significantly lower than from the other sources. Therefore, we will not compensate it and leave it for further study.

The histograms suggest that majority of the deviation is close to zero; however, the distribution appears to have too many distant realizations to be considered as being Gaussian. Therefore, we will model these deviations as uniformly distributed on a symmetric interval around zero with bounds given by the maximum observed value of the deviation. Contribution of this error to e_t is then obtained using Remark 1 as follows: $Q_{discr} = \mathrm{diag}(8e{-}6, 8e{-}6, 5e{-}7, 3e{-}13)$.

Impact of unknown load torque

Temporal variation of the load torque (T_L) can be slower than the sampling period, hence it can not be considered to be a white noise. The load torque represents a systematic error in (3). Therefore, we will analyze two approaches to this problem: (i) direct estimation of T_L, and (ii) derivation of contribution from unknown T_L to disturbances e_t in the same spirit as in the previous Section.
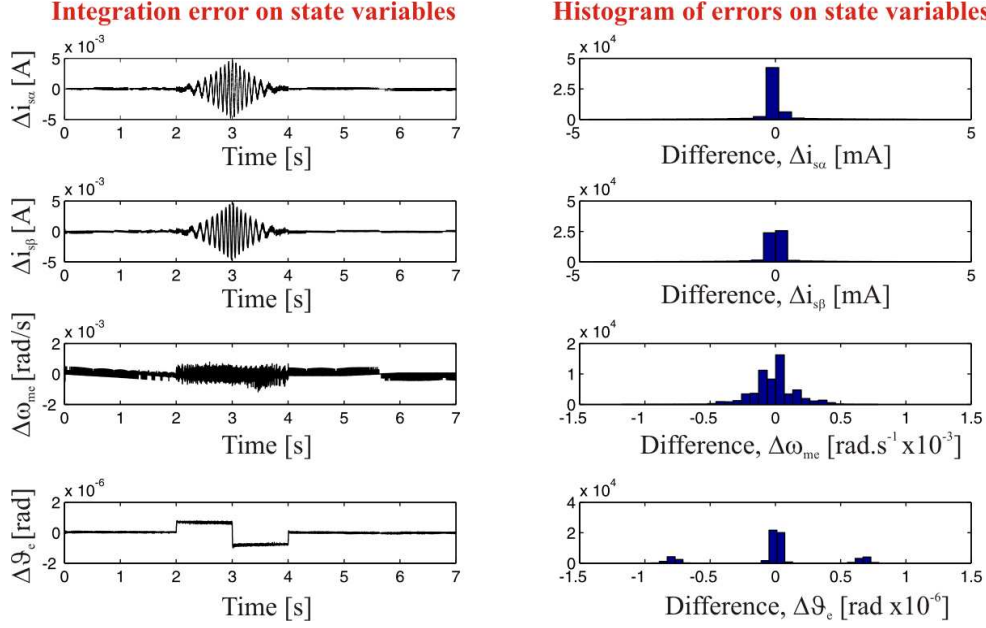
Fig. 4 Deviation of the state space model (3) from continuous-time solution of model (1), displayed for each state variable in each row, respectively. **Left**: evolution of deviation in time. **Right**: histograms of the deviation. Data source: simulator; speed profile; no-load motor.

Estimation of the load torque

In order to estimate T_L we must model its evolution in time. We consider a Gaussian random walk:

$$T_{L,t} = T_{L,t-1} + e_{T,t}, \quad p(e_{T,t}) = N(0;q_T),\qquad(7)$$

where variance parameter q_T governs tightness of the walk. This is a free parameter, the influence of which will be studied in simulation. The new state is $x_t = [i_{s\alpha}; i_{s\beta}; \omega_{me}; \vartheta_e; T_{L,t}]$ with covariance matrix of disturbances $Q = \mathrm{diag}(q_{pwm}+q_{d1}, q_{pwm}+q_{d2}, q_{d3}, q_{d4}, q_T)$. This model will be denoted by EKF TL.

Propagation of load torque in stochastic model

In some applications, further extension of the state-space is prohibited, e.g. for computational complexity reasons. In that case, the load torque can be considered as a disturbance which propagates through (3) and influences all elements of covariance matrix Q. This can be achieved using Schmidt-Kalman filter [10]. In this paper, we apply a simpler heuristic approach based on propagation of the unknown contribution of T_L in the third equation of (3) to the remaining equations. First, T_L will affect the third equation in (3) such that the difference between ω_{me} computed with known T_L and ω_{me} computed for $T_L = 0$ is $\Delta\omega = -p/J\, T_L\Delta t$. This difference will be propagated to the remaining equations via substitution of $\omega_{me} + \Delta\omega$ in place of ω_{me}, causing differences:

$$\Delta i_{s\alpha}(t+1) = +\frac{\Psi_{PM}}{L_s}\Delta t\Delta\omega\sin\vartheta_e(t)$$

$$\Delta i_{s\beta}(t+1) = -\frac{\Psi_{PM}}{L_s}\Delta t\Delta\omega\cos\vartheta_e(t)\qquad(8)$$

$$\Delta\vartheta_e(t+1) = +\Delta t\Delta\omega.$$

Since functions sin() and cos() are bounded, the maximum absolute value of error on the first two equations is $|\Delta i_{s\alpha,\beta}| = \Psi_{PM}/L_S\, p/J\, T_L\Delta t^2$, $|\Delta\omega| = p/J\, T_L\Delta t$ on the third equation, and $|\Delta\vartheta| = \Delta t\Delta\omega$ on the fourth. These values can be converted to contributions to covariance matrices Q_{TL} using Remark 1. However, since these differences are systematic (i.e. they do not have zero mean) the deviation may not be sufficiently compensated by the EKF and it can grow with time. Thus, we propose to increase Q_{TL}, by a multiplicative constant $c_{TL} > 1$. We do not provide any guidance how to choose c_{TL} – it remains to be done experimentally. However, it is the only parameter that must be tuned which is much easier than tuning the full covariance matrix. This model will be denoted by EKF PTL.

Theoretical limits of model accuracy

The developed covariance matrices determine theoretical limits of accuracy of any estimator based on this model. These limits are known as Cramer-Rao bounds on minimum mean-square error. These bounds can be computed recursively using all possible realizations of the random process [11]. However, disturbances of the model in our case are not stochastic. Repeated runs of the simulator will result in the same trajectory of the system. It is easy to show that the Cramer-Rao bound is equal to covariance matrix P of the posterior state density if the EKF is evaluated exactly in the simulated state. For illustration, the Cramer-Rao bounds for both variants of the stochastic model (i.e. EKF TL and EKF PTL) are displayed in Fig. 5.

Note that the Cramer-Rao bound on position is almost equal for both considered variants of the model. In fact, the most significant influence on it have values $Q_{1,1}$ and $Q_{2,2}$ which are equal for both models. The bound however reveals principal properties of the model. Namely, for non-zero speed the uncertainty on position is proportional to the speed (compare time intervals of 2-3s with 7-9s), for zero speed (standstill) the uncertainty in position is linearly increasing.
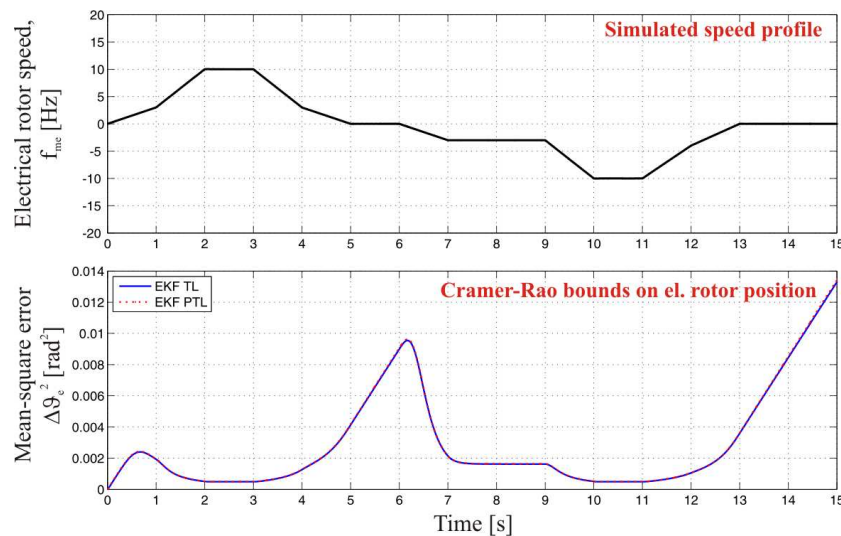

Fig. 5   Cramer-Rao lower bounds on mean-square error of estimates of rotor position (bottom) for a simulated speed profile (top). Data source: simulator.

Verification of the model on real data

Validity of the presented stochastic model was tested on real data recorded on the prototype of PMSM drive of rated power of 10.7kW. We have recorded many transients on the drive on which we have then off-line tested the proposed EKF estimator. The components of both the demanded stator voltage vector ($u_{s\alpha\_eqv}$ and $u_{s\beta\_eqv}$) commanded by DSP (see next section for detail description of the configuration of designed drive prototypes) and the stator current vector ($i_{s\alpha}$ and $i_{s\beta}$) were transformed from the digital form to the analog via a D/A converter installed in the drive controller. The output of the D/A converter has been recorded by a 4-channel digital scope TEKTRONIX MSO4054. The data from the scope has been stored in a CSV file which served as a data source for off-line testing of our simulator. The rotor speed and position measured by the rotor position sensor as well as components of the stator current vector have been simultaneously recorded by the PC-based master control unit of the drive. Results of one of the tests are presented in Fig. 6. The data were recorded during the drive start-up and speed reversals – triangular speed profile, commanded electrical rotor speed of ±5Hz. The EKF TL estimator provides additional estimate of the load torque which in effect compensate additional inaccuracies of the model (see Fig. 6, bottom).

Sensorless Controlled PMSM Drive Prototypes: Experimental Results and Simulator Verification

We are aware that the simulation model has always some deviations from an original physical object. Therefore, we have carefully calibrated our simulator and verified it using two servo drives with PMSM of rated power of 10.7kW and 310W on which we have made extensive experimental tests.

The control strategy presented in Fig. 2 has been implemented in a fixed-point digital signal processor Texas Instruments TMS320F2812. EKF has been implemented in DSP in a form of manually optimized equations which strongly reduced requirements on both computation performance and memory space. Computation of EKF takes 78μs with DSP clock frequency of 150MHz.

Presented simulation and experimental results use carrier-based PWM with injected third harmonic component with carrier frequency of 4kHz. Sampling period of vector control as well as of the EKF has been selected of 125μs. Fig. 7 demonstrates results of developed drive simulator and presents behavior of sensorless controlled drive of rated power of 10.7kW under speed reversal transient. We have employed a triangular speed profile with electrical rotor speed commands of ±100Hz. We have selected quite slow speed ramp in order to verify proper function of the drive in critical low speed region. Fig. 8 displays experimental results introducing the same transient effect as in Fig. 7. Behavior of designed PMSM drive prototype of 310W is documented in Fig. 9 which analyzes speed reversal transient under sensorless control mode. In this test, we have utilized a trapezoidal speed profile with electrical rotor speed commands of ±50Hz. The carrier frequency of the PWM has been in this case of 8kHz while the sampling period of both the controller and the EKF stayed unchanged, i.e. 125μs.
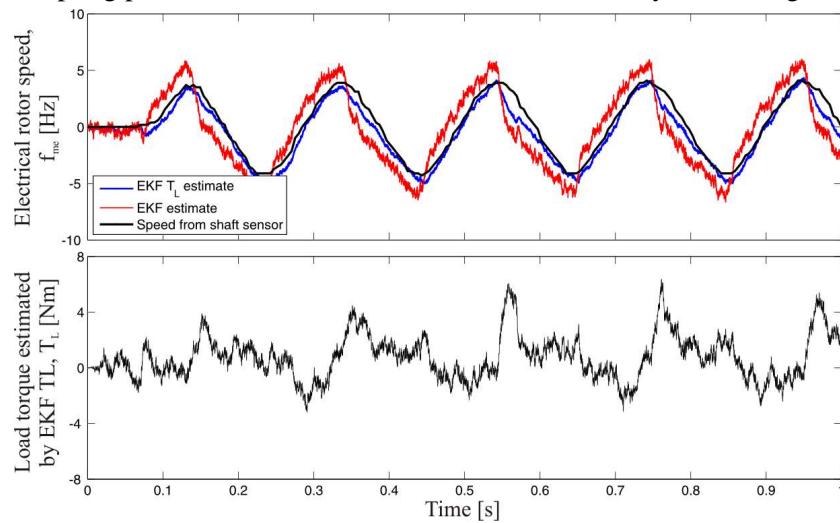

Fig. 6   Comparison of measured el. rotor speed with estimates provided by EKF TL and EKF (**top**). **Bottom**: load torque estimated by EKF TL. Data source: real data recorded on 10.7kW drive prototype; drive start-up and speed reversals – triangular el. rotor speed profile of ±5Hz.

Conclusion & Discussion

The sophisticated simulator of permanent magnet synchronous machine (PMSM) drive was developed using Bayesian Decision Making (BDM) environment. This simulator has been used to study the influence of various uncertainties as a disturbance in conventional model of PMSM drive. Stochastic properties of these disturbances were summarized and used for tuning of covariance matrices of the EKF by the presented semi-analytical approach. Very important task has been improvement of the stochastic drive model. We have focused on two particular problems: (i) improved reconstruction of the stator voltage vector, and (ii) modeling of unknown load torque. The theoretical results have been verified by tests on two PMSM drives prototypes of rated power of 10.7kW and 310W. Experimental testing covered both on-line tests on designed drive prototypes and off-line tests using data recorded on these drives as the data source in the simulator. The proposed stochastic model extends operating speed range of the drive, however, there are still serious constrains of the EKF estimator.

The main problem of EKF based estimator is that this filter does not guarantee convergence if the operating point is far from the true state. Moreover, the underlying stochastic model has a singular point at zero speed which has been demonstrated using Crammer-Rao bounds. These properties strongly limit applicability of this estimator. The prospective way for overcoming of above mentioned limits could be application of estimator employing higher number of operating points such as interacting multiple models or particle filters. Furthermore, the Gaussian representation of the uncertainties does not exactly respect the physical reality. Hence, the new solutions should take advantage of non Gaussian noise models which better corresponds with the reality.
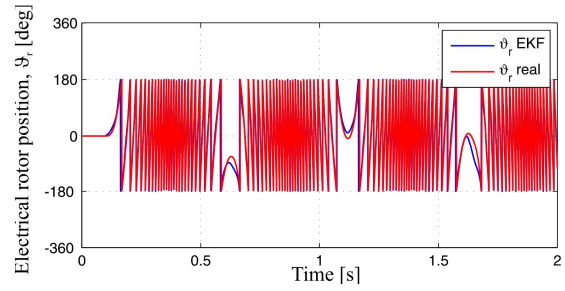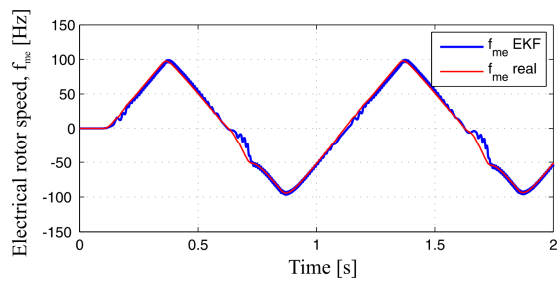
Fig. 7: Simulation results – sensorless drive operation – drive 10.7kW: speed reversal, triangular speed profile, commanded el. rotor speed of ±100Hz
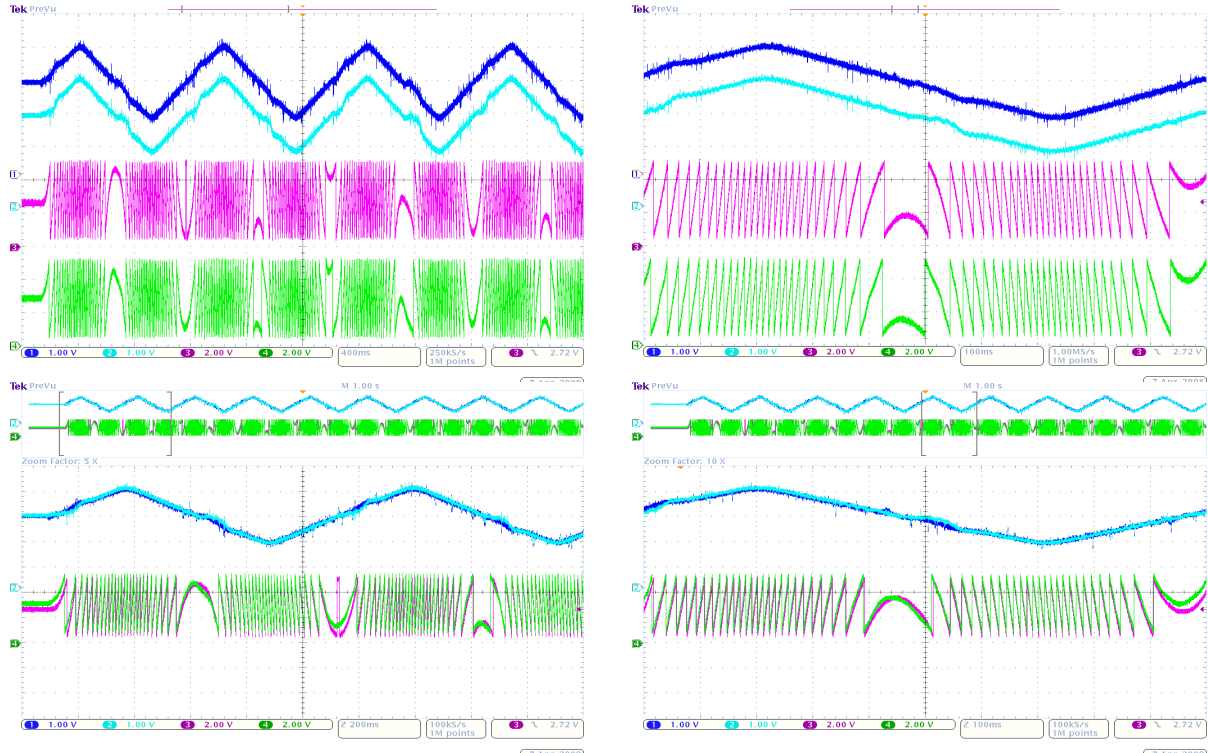

Fig. 8: Sensorless drive operation – drive of 10.7kW: speed reversal – triangular speed profile, commanded el. rotor speed of ±100Hz, ch1: el. rotor speed – sensor (80Hz/V), ch2: EKF estimated el. rotor speed (80Hz/V), ch3: electrical rotor position – sensor (72deg/V), ch4: EKF estimated el. rotor position (72deg/V)
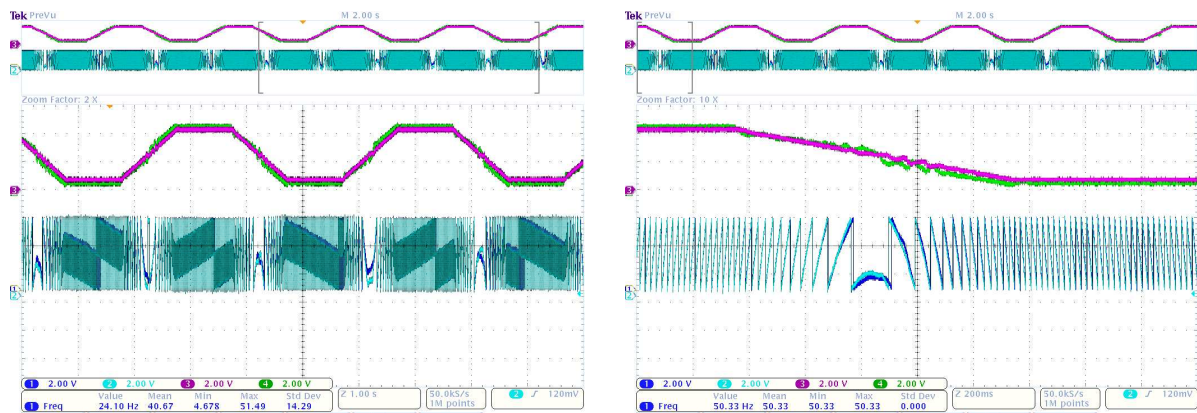

Fig. 9: Sensorless drive operation – drive of 310W: speed reversal – trapezoidal speed profile, commanded el. rotor speed of ±50Hz, ch1: electrical rotor position – sensor (72deg/V), ch2: EKF estimated el. rotor position (72deg/V), ch3: el. rotor speed – sensor (25Hz/V), ch4: EKF estimated el. rotor speed (25Hz/V)

References

[1] Vas, P.: Sensorless Vector and Direct Torque Control. Oxford University Press, New York, USA, 1998.

[2] Dhaouadi, R.; Mohan, N.; Norum, L.: Design and Implementation of an Extended Kalman Filter for the State Estimation of a Permanent Magnet Synchronous Motor. IEEE Transactions on Power Electronics, Vol. 6, No. 3, July 1991, pp. 491 – 497.

[3] Bolognani, S.; Zigliotto, M.; Zordan, M.: Extended-Range PMSM Sensorless Speed Drive Based on Stochastic Filtering. IEEE Trans. on Power Electronics, Vol. 16, No. 1, January 2001, pp. 110 – 117.

[4] Vaidyanathan, C.; Kettle, P.; Moynihan, F.; Lehman, B.: Highly Flexible Motor Control Possible for the Appliance Market. In EPE 1999, Lausanne, Switzerland, 1999.

[5] Peroutka, Z.: Design Considerations for Sensorless Control of PMSM Drive Based on Extended Kalman Filter. In EPE 2005, Dresden, Germany, 2005.

[6] Park, P.; Kailath, T.: New Square-Root Algorithms for Kalman Filtering. IEEE Transactions on Automatic Control, Vol. 40, No. 5, May 1995, pp. 895 – 899.

[7] Ristic, B.; Arulampalam, S.; Gordon, N.: Beyond the Kalman Filter: Particle Filters for Tracking Applications. Artech House Publishers, 2004.

[8] Doucet, A.; De Freitas, N.: Sequential Monte Carlo Methods in Practice. Springer, 2001.

[9] Holtz, J.: Sensorless Vector Control of Induction Motors at Very Low Speed Using a Nonlinear Inverter Model and Parameter Identification. IEEE Transactions on Industry Applications, VOL. 38, NO. 4, JULY/AUGUST 2002. pp. 1087 – 1095.

[10] Grewal, M.S.; Andrews, A.P.: Kalman filtering: theory and practice using MATLAB.Wiley New York,2001

[11] Tichavsky, P., Muravchik, C.H. and Nehorai, A., "Posterior Cramer-Rao bounds for discrete-time nonlinear filtering". IEEE Transactions on Signal Processing, Vol. 46, No. 5, 1998, pp. 1386–1396.